OPEN ACCESS Freely available online

PLOS ONE

Correlation between Histopathological and FT-Raman Spectroscopy Analysis of the Liver of Swiss Mice Infected with *Paracoccidioides brasiliensis*

Elaine Sciuniti Benites Mansano[1], Gutierrez Rodrigues de Morais[2], Edilaine Martins Moratto[1], Francielle Sato[2]*, Antonio Medina Neto[2], Terezinha Ines Estivalet Svidzinski[3], Mauro Luciano Baesso[2], Luzmarina Hernandes[1]

1 Department of Morphological Sciences, Universidade Estadual de Maringá, Maringá, Paraná, Brazil, **2** Department of Physics, Universidade Estadual de Maringá, Maringá, Paraná, Brazil, **3** Department of Clinical Analysis and Biomedicine, Universidade Estadual de Maringá, Maringá, Paraná, Brazil

Abstract

Paracoccidioidomycosis is the most important systemic mycosis in Latin America. The main entrance of the fungus is the airway. It primarily occurs in the lung, but in its disseminated form may affect any organ. The liver is one of the organs afflicted by this disease and its homeostasis may be impaired. The aim of the present study was to evaluate the evolution of paracoccidioidomycosis in the liver of Swiss mice and correlate morphological factors with the expression of gp43 and with physicochemical analysis via FT-Raman of the infected organ. According to colony forming unit (CFU) and granuloma counting, the first and second weeks were the periods when infection was most severe. Tissue response was characterized by the development of organized granulomas and widespread infection, with yeasts located within the macrophages and isolated hepatocytes. The gp43 molecule was distributed throughout the hepatic parenchyma, and immunostaining was constant in all observed periods. The main physicochemical changes of the infected liver were observed in the spectral ranges between 1700–1530 cm^{-1} and 1370 – 1290 cm^{-1}, a peak shifting center attributed to phenylalanine and area variation of -CH_2 and -CH_3 compounds associated to collagen, respectively. Over time, there was a direct proportional relationship between the number of CFUs, the number of granulomas and the physicochemical changes in the liver of mice infected with *Paracoccidioides brasiliensis*. The expression of gp43 was similar in all observed periods.

Citation: Mansano ESB, Morais GRd, Moratto EM, Sato F, Medina Neto A, et al. (2014) Correlation between Histopathological and FT-Raman Spectroscopy Analysis of the Liver of Swiss Mice Infected with *Paracoccidioides brasiliensis*. PLoS ONE 9(9): e106256. doi:10.1371/journal.pone.0106256

Editor: Kirsten Nielsen, University of Minnesota, United States of America

Received April 21, 2014; **Accepted** August 1, 2014; **Published** September 2, 2014

Data Availability: The authors confirm that all data underlying the findings are fully available without restriction. All relevant data are within the paper.

Funding: This study received financial support from Brazilian agencies Fundação Araucária and CNPq, under the Project PRONEX 114/2010 – "Nucleus of Excellency in Advanced Optics for Biophysical and Biomedical Applications". The funders had no role in study design, data collection and analysis, decision to publish, or preparation of the manuscript.

Competing Interests: The authors have declared that no competing interests exist.

* Email: fsato@uem.br

Introduction

Paracoccidioidomycosis (PCM) caused by *Paracoccidioides spp.* is endemic in humid tropical and subtropical areas of Latin America where it is considered one of the most important mycoses and, among chronic infectious and parasitic diseases, represents the eighth leading cause of death from infectious disease. It has the highest mortality rate among systemic mycoses [1–3]. It is granulomatous in character and grows insidiously. It is of considerable medical importance, as it affects people in their productive phase, making them unable to work and resulting in sequelae [4,5].

Paracoccidioides brasiliensis (Pb) is the main agent of PCM. It is a thermally dimorphic fungus: it appears as mycelium at 25°C and as yeast at 36°C [6]. In yeast form it can spread through the body of the host and parasite deeper tissues [7,8]. The occurrence of yeasts within polymorphonuclears, monocytes and macrophages shows that this strain can survive within these cells [9].The principal antigenic component of Pb is a 43 kDa glycoprotein known as gp43 [10] which is synthesized and transported to the cell wall and then secreted to the medium [11]. There is evidence that gp43 participates in adhesion, invasion and pathogenesis of the fungi [12], inhibits the fungicidal activity of macrophages, and contributes to the development of infection in susceptible hosts [13]. Additionally, gp43 is the main known antigen for the diagnosis and prognosis of PCM [14]. Diagnosis of natural PCM is currently based on the appearance of the agent in tissue. However, this diagnostic process is limited, and serological techniques have been proposed as an alternative [15,16].

A new perspective for the diagnosis of PCM is via Fourier Transform Raman Spectroscopy (FT-Raman). This technique allows the characterization of molecular components and detects, by the Raman bands, structural deformations resulting from infection [17]. In fact, infrared methods can accelerate the diagnosis of diseases and represent a breakthrough in experimental investigations of PCM [18,19].

The main organ affected by PCM is the lung, but can often affect other sites such as bone, skin, mucosa and lymphoid organs [2,3,20]. The liver can also be affected by this disease, and some studies show that liver enzymes are altered [21,22] indicating that

the infection can disrupt the homeostasis of this organ. However, there are no studies of the liver of animals infected with Pb using FT-Raman spectroscopy.

The aim of this study was to evaluate the morphological evolution of paracoccidioidomycosis in the liver of *Swiss* mice and to correlate morphological changes with the expression of gp43 and with physicochemical analysis of the infected organ using FT-Raman spectroscopy.

Materials and Methods

Fungal Isolate

A sample of *Paracoccidioides brasiliensis* (Pb 18 isolate) was obtained from the Fungal Culture Collection of the Department of Immunology of the Universidade Federal de São Paulo (UNIFESP) and stored in Fava Neto culture medium at 35°C in the Medical Mycology laboratory of the Universidade Estadual de Maringá (UEM).

Animal Experimentation

All procedures involving animals were approved by the Ethics Committee in Animal Experimentation (CEEA) of the Universidade Estadual de Maringá, under register number 116/2010.

A total of 32 *Swiss* male mice, weighing 30 g and aged between 4 and 5 weeks, were used. The animals were transferred from the Central Animal Laboratory to the Laboratory for Paracoccidioidomycosis Experimentation of the Department of Basic Health Sciences. The animals were kept under controlled environmental conditions, with a temperature of 23–24°C, and a light/dark cycle of 12 hours with free access to water and food.

Infection of animals with *Paracoccidioides brasiliensis* fungal isolate

The mice were divided into four groups of eight, six of which were infected and two were used as control. The animals were anesthetized by intramuscular injection of a solution containing 100 mg/kg of ketamine hydrochloride (Park, Davis & Company, Berlin, Germany) and 10 mg/kg xylazine (Bayer, Brazil) [23]. After the anesthesia the mice were infected, via the lateral tail vein, with 0.1 ml of a fungal suspension containing 2×10^6 yeast cells of Pb per milliliter of colony forming units (CFU/ml). Control animals received 0.1 ml of sodium phosphate buffer (PBS), pH 7.4, in the same manner.

Death of animals

Animals from both infected and control groups were killed 1, 2, 4 and 8 weeks after inoculation, with an overdose (40 mg/kg) of sodium thiopental (Crystal Pharma, Minas Gerais, Brazil) in the lateral tail vein. The liver was removed and the right lobe was isolated and fixed in 4% paraformaldehyde solution for 24 hours and processed for paraffin embedding. Five mm thick semi-serial cuts were made. Fragments of the left lobe were weighed and placed in sterile test tubes with 1 ml of PBS then macerated with a pistil to obtain a homogenous suspension. This suspension was used for counting the CFUs. The remainder of the left lobe was used for spectroscopic study by FT-Raman.

Identification of CFUs/g of liver tissue

A volume of 300 µl of the infected liver suspension was placed in Petri dishes containing brain heart infusion (BHI) agar medium (Difco Laboratories, Detroit, Michigan) supplemented with 5% fetal bovine serum and growth factors [24]. The plates were incubated at 35°C for 15 days. CFUs/g counting was performed on the seventh and fifteenth days of incubation and the $\log_{10}$ of the CFUs/g was calculated.

Histological and immunohistochemical study

Histological sections of liver were stained with: (a) hematoxylin and eosin (H&E) and (b) periodic acid-Schiff (PAS) for histopathological evaluation; (c) sirius red by picrosirius technique to assess the presence of fibrosis; (d) impregnated by silver-methenamine in accordance with Gomori-Grocott and counter-stained with light green or H&E [25,26] for locating the yeast in the hepatic parenchyma; and (e) immunostained with anti-gp43 antibody to detect expression of the glycoprotein gp43.

Expression of gp43 in the liver was detected by avidin-biotin peroxidase immunohistochemical staining method using polyclonal primary antibody, anti-gp43 obtained in rabbits, and diluted in a concentration of 1:50, and revealed using a immunohistochemical commercial kit (Histostain-Plus kits, Invitrogen 2nd Generation, LAB-AS Detection System, Camarilo, CA).

Slides were observed and photographed using a trinocular light microscope (Nikon Eclipse 80i), with a camera (Nikon DSFi1C) coupled to a computer using Nis Element software (Shinjuku, Japan).

Granuloma Counting

Granuloma counting was performed in histological sections stained with H&E. Granulomas present were counted in four histological/animal sections (24 sections/week of infection).

A histological section of the liver was outlined in order to create a chart that plotted the positions of the granulomas found in all of the sections analyzed, thereby avoiding repeated counts of the same granuloma. The counts were carried out using a 20× objective on a microscope (Nikon Eclipse 80i).

To determine the approximate area in which the counting was carried out, the image of histological section of the liver of each animal was captured and its area determined using an image analysis program (Image Pro Plus, version 4.5). A mean area of (15.25 ± 0.85) mm^2 was calculated and used as a standard for the area in which the granulomas were counted. The numbers of granulomas were therefore expressed as number of granulomas/ 15.25 mm^2.

Fourier Transform Raman Spectroscopy (FT-Raman)

The analysis was performed on a FT-IR spectrometer coupled to a Raman module (Vertex 70 – RAM II module, Bruker, Germany), equipped with a Nd-YAG laser excitation source at 1064 nm and a germanium detector cooled to liquid nitrogen. The power used was 70 mW. Liver samples with a surface area of approximately 1 cm^2 were analyzed in the spectral range between 3300 – 1200 cm^{-1}. The spectra obtained for each sample represented an average of 400 scans with spectral resolution of 4 cm^{-1}. The analyzed areas for all samples were the same since the adopted diameter for the excitation laser spot was around 4 mm.

Statistical Analysis

Variance analysis (ANOVA) was performed to assess the number of CFUs/g and of granulomas, using Graph Pad Prism 3.0 software (Graph Pad Software, Inc., La Jolla, CA, USA). The Tukey post-test was used with a 95% confidence level.

Results

1. Counting of Colony Forming Units - CFUs

The number of CFUs of the fungus found in the liver of the animals decreased after the first week, with a significant reduction between the 4th and 8th weeks of infection (Figure 1).

2. Granuloma Counting

The granuloma counting results are shown in Figure 2. The granulomatous lesions decreased between the second and fourth weeks but remained constant in the other periods.

3. Histopathological Study

In the first weeks of observation, the formation of granulomas was one of the most obvious changes in the hepatic parenchyma of infected mice.

In the first week (Figure 3) the granulomatous lesions occurred predominantly in the periphery of the organ. They appeared as well-defined structures consisting of aggregates of histiocytes, macrophages, plasma cells, lymphocytes and neutrophils. In this period, the yeasts were evident with their characteristic morphology within the granulomas, and could be viewed only with Grocott-Gomori staining. Eventually, isolated macrophages and hepatocytes revealed impregnation by silver. Other histological changes such as the presence of mitosis and eosinophilic cytoplasm of the hepatocytes were observed in the first week of infection, the period in which the largest number of CFU (2.05 CFU/$\log_{10}$) occurred (Figure 1).

In the second week (Figure 4) liver disease presented two morphological patterns: (1) areas with organized granulomas well defined, containing yeast, interspersed with areas of normal parenchyma, and (2) other areas with diffuse infection without clear limits where the hepatic parenchyma had necrotic areas with cytoplasm acidophilic, pyknosis and nuclear chromatolysis. In these regions, the yeasts appeared isolated, intact or fragmented within hepatocytes. Fragmented yeasts impregnated by silver were identified within macrophages. A total of 100% of the samples revealed yeast, with or without budding.

Sections after four and eight weeks of infection (Figure 5) showed morphological features similar to those described for previous weeks, but in reduced proportions (fewer granulomas, reduced extent of lesions and fewer CFUs). At the same time the number of animals with granulomatous lesions also varied (77% in the fourth week and 50% in the eighth week). The eighth week had the lowest number of CFUs.

There was an increase over time in the amount of collagen fibers concentrated close to the sinusoidal capillaries between the hepatic cords (Figure 6).

Anti-gp43 expression occurred in both regions; nuclear and cytoplasmic of the hepatocytes presenting an imunostaining diffuse

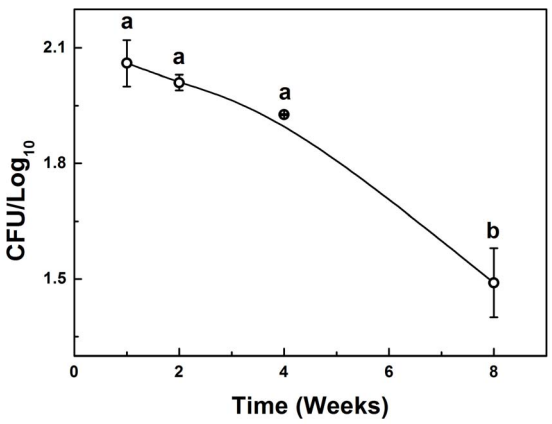

Figure 1. Number of Colony Forming Units (CFUs)/g in the liver of mice infected with *Paracoccidioides brasiliensis*. Results represent mean ± EPM and were expressed as Log_{10}; n = 6. Different letters represent P<0.001. ANOVA, Tukey post-test.
doi:10.1371/journal.pone.0106256.g001

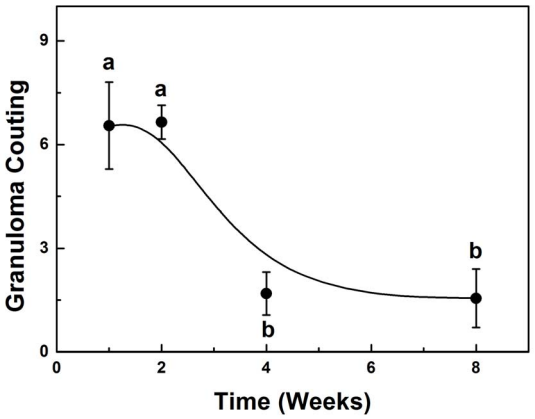

Figure 2. Number of granulomas in the liver of mice infected with *Paracoccidioides brasiliensis* as a function of time infection. Results expressed as the mean ± EPM. Different letters represent P< 0.001. ANOVA, Tukey post-test.
doi:10.1371/journal.pone.0106256.g002

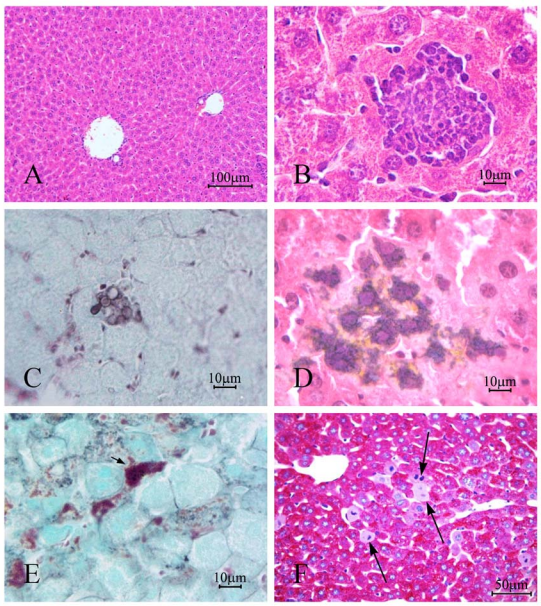

Figure 3. Photomicrograph of: (A) liver of mice control, non-infected and (B - F) after one week of infection with *Paracoccidiodes brasiliensis*. In (B) yeasts were not observed in the stained granulomas with H&E, though sprouting and varied shapes were indentified with (C) Gomori-Grocott staining; in (D) and (E) note the presence of fungical fragments impregnated with silver within hepatocytes and macrophages (arrow); in (F) large number of mitosis (arrow) were observed in the hepatic parenquima. Stain: H & E (A and B); Gomori-Grocott counter-stained with green light (C and E) or H & E (D); Periodic acid-Schiff (PAS)(F).
doi:10.1371/journal.pone.0106256.g003

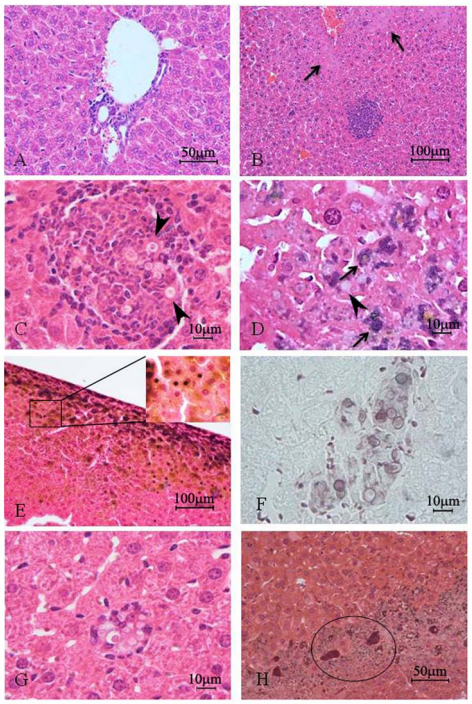

Figure 4. Photomicrograph of: (A) liver of mice control, non-infected and (B-H) after two weeks of infection with *Paracoccidiodes brasiliensis*. The hepatic parenchyma showed more developed granulomas (B and C) and more eosinophic areas (arrows) (B); the yeast were visualized inside the H&E stained granulomas (C); the hepatic parenchyma showed intracytoplasmic fungal fragments (arrows) and karyolysis (D); the infection was more evident in the organ periphery where several pyknotic nuclei were identified (E); the granulomas showed high number of yeast (F); in this period large macrophages with yeast inside (circled area) (G) and large necrotic areas (H) were observed. Stain: H&E (A, B, C and G); Gomori-Grocott counter-stained with H&E (D, E and H) or green light (F).
doi:10.1371/journal.pone.0106256.g004

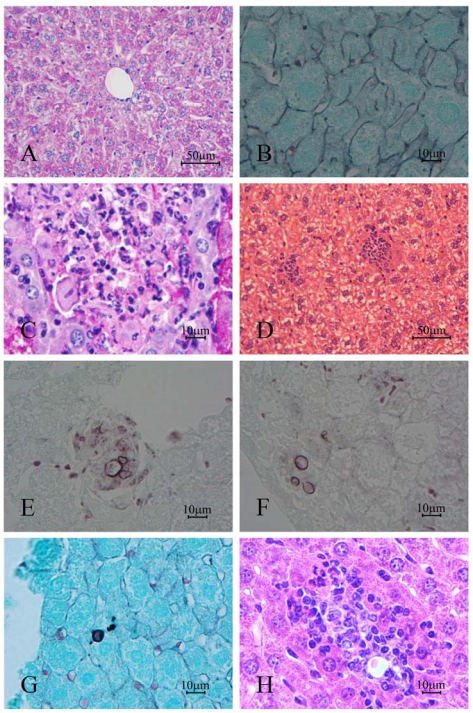

Figure 5. Photomicrograph of: (A and B) liver of mice control, non-infected and (C - F) after four (G and H) and eight weeks of infection with *Paracoccidiodes brasiliensis*. Organized granulomas (C) with a fewest or without yeasts (C-F) were observed on the fourth week. On the eighth week yeasts were still observed. Stain: Periodic acid-Schiff (PAS) (A and C); Gomori-Grocott counter-stained with green light (B and E-F) or H&E (D and H).
doi:10.1371/journal.pone.0106256.g005

pattern. Yeast with marking was rarely seen. Instead, large areas were immunostained throughout the parenchyma. The staining was similar in all the observed periods (Figure 6).

4. Physicochemical analysis by Fourier Transform Raman Spectroscopy

The results show that there are spectral differences in the liver of mice infected with Pb compared to those of normal mice (Figure 7).

The functional groups associated to each numbered peeks and their respective attributions are shown in Table 1 and Figure 7 (A). All spectra were subjected to baseline correction and normalized with regard to the peak of the amide I (1660 cm^{-1}). Figures 7 (B) and 7 (C) shows the regions in which Gaussian fitting, for obtaining the position and area of the characteristic peaks of infected and non-infected tissue, were performed. Figure 7 (C) shows the spectra between 1370-1290 cm^{-1}, associated with the deformation of -CH_2 and -CH_3, and in this region there was a variation in the area with increased time of infection. The functional groups, -CH_2 and -CH_3 are usually correlated to the presence of collagen fibers in the tissues [27–29]. This variation was investigated using the ratio between the area of the collagen and amide III regions (1260 cm^{-1}), a nearby region to the collagen, which remains stable during the studied time of infection. The results are presented in Figure 8 in which the behavior of this ratio comparing the control (t = 0) with the infected liver after one, two, four and eight weeks, showing a decay of the collagen area in the first two weeks, followed by an increase after the fourth week of infection.

Figure 9 (A) shows the peak displacement of 1615 cm^{-1} identified in the spectrum of the control liver toward lower frequencies as a function of infection time, reaching a value of 1595 cm^{-1} in the eighth week. This region can be related to amino acids in the liver itself or in the blood. The peak at 1615 cm^{-1} is attributed to tyrosine [27,28] and at 1585 cm^{-1} to phenylalanine [27,28]. Figure 9 (B) shows the behavior of the total area related to these amino acids (1710-1510 cm^{-1}) as a function infection time.

There is a decrease in the amino acids content in the first week of infection compared to control tissue and a tendency of increasing up to the eighty week. From the second week on there is a tendency to increase the total area of the amino acids. However it should be considered that the greatest contribution in the control liver is due to the presence of tyrosine, and for the infected tissue it is from the phenylalanine.

Discussion

In this study, FT-Raman technique and histological staining were used to assess the behavior of the liver infected with Pb from a morphological and physicochemical perspective. The expression over time of the major antigen produced by Pb, gp43, was assessed.

In natural PCM the liver is not the preferred organ, but it is affected from the pulmonary focus after fungal spreads via

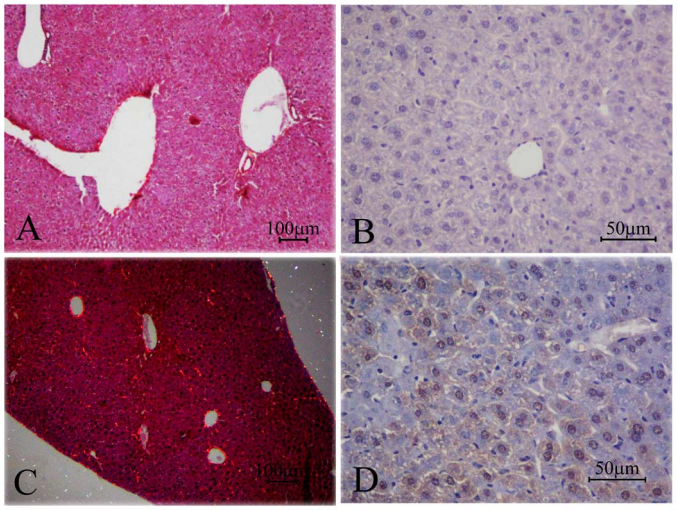

Figure 6. Photomicrograph of: (A and B) liver of mice control, non-infected and (C and D) after eight weeks of infection with *Paracoccidiodes brasiliensis*. Note an increase in the number of birefringent collagen fibers (C). Immunhistochemistry using anti- gp43 antibody showed diffuse cytoplasmic and nuclear staining in the liver parenchyma (D). Stain: Picrosirius technique (A and C); Avidin-biotin peroxidase immunohistochemical using anti-gp43 antibody (B and D).
doi:10.1371/journal.pone.0106256.g006

lymphatic and hematogenous route [30,31,2]. In comparison with studies of lungs, there are few clinical and experimental studies describing the involvement of the liver. Hepatosplenomegaly, jaundice and fibrosis are some of the described pathological alterations in patients infected with Pb [32–34]. However, it is important to mention that in the acute form of the PCM, that affects mainly children's and teenagers, the liver is between the most affected organ [35,36].

In this study the intravenous route of infection of the Pb strain, one of the most virulent forms of Pb, seemed to promote the spread of the fungus and its installation in the liver. The infection was confirmed by CFU analysis, where fungal growth was evaluated.

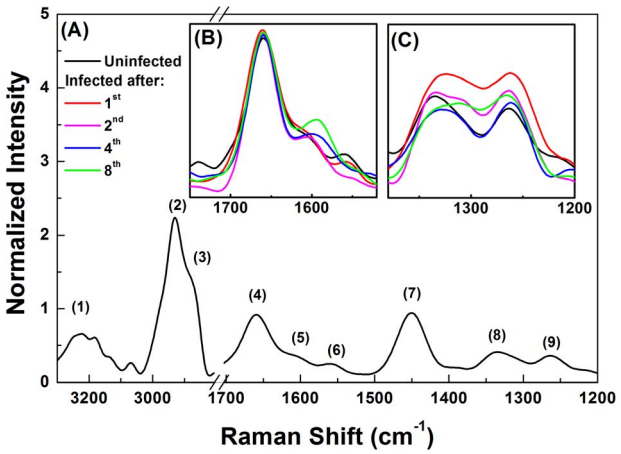

Figure 7. Raman spectrum from liver of mice (A) control, non-infected and (B and C) after one, two, four and eight weeks of infection with *Paracoccidioides brasiliensis*. The insets show the spectral range between 1750-1520 cm^{-1} (B) and 1380-1200 cm^{-1} (C) where the spectral difference compared non-infected with infected tissues were observed.
doi:10.1371/journal.pone.0106256.g007

Histopathological study using serial sections stained using different techniques proved, from different perspectives, the host-parasite relationship and the changes in the liver morphology. Hematoxylin and eosin staining and PAS technique identified granulomas containing yeast forms of Pb with clear halo and central acidophilic regions. Silver impregnation showed yeasts within the inflammatory infiltrate [37] and in the parenchyma of the liver.

In the liver stained in accordance with Gomori-Grocott, the structures impregnated by silver were located internalized within cells that were predominantly at the periphery of the liver, near the visceral peritoneum. These cells were identified as macrophages, because of their irregular shape and variable position, which suggests that these cells engulfed the yeasts to kill them, or that there were yeasts resident in these macrophages. Many hepatocytes also had small intracytoplasmic structures impregnated with silver, suggestive of internalized micro yeasts.

The method by which Pb can spread to organs is not fully understood. One way may be by migration of infected macrophages or dendritic cells through the lymph system [38,39]. Yeasts have been found intracellularly in polymorphonuclear cells and in monocytes and macrophages, suggesting that the fungus is able to survive within these cells [9,40], and can therefore remain hidden into the immune defenses of the host. It does not expose its antigen on the surface cell, escaping from professional phagocytes, facilitating therefore its dissemination [41].

In the present study, the number of fungi in the lesions decreased in the later periods of infection, suggesting that the granulomas formed in the first weeks represented an initial defense mechanism against Pb, affecting the multiplication and spread of yeast. It is possible that the more compact architecture of the liver, with few open spaces, may have hindered the establishment and spread of the fungus throughout the parenchyma, compared with the lung [37], which has ample space.

Moreover, it is possible that the mice developed a hyperergic form of the disease with cellular type immune response forming well-organized granulomas with few fungi, suggesting that these animals have high immunological resistance. Other authors have

Table 1. Non-infected mice liver Raman bands and its assignments.

Peak N°	Raman shift (cm^{-1})	Band assignments
1	3220	v(N-H) (Protein related) [57]
2	2927	v_{as}(C-H) (Lipids and protein related) [27]
3	2874	v_s(C-H) (Lipids and protein related) [27]
4	1660	Amide I (Protein related) [29]
5	1615	Tyrosine (amino acid) [28]
6	1557	δNH_3^+) (Red cell blood contribution) [27,58]
7	1450	$\delta(CH_2)$ (Lipids and protein related) [27]
8	1340	$\delta(CH_2)$ and δ (CH_3) (Collagen)[27,29]
9	1260	Amide III [27,28]

v: stretching vibration; v_{as}: asymmetric stretching vibration; v_s: symmetric stretching vibration; δ_{as}: asymmetric bending vibration; δ_s: symmetric bending vibration.
doi:10.1371/journal.pone.0106256.t001

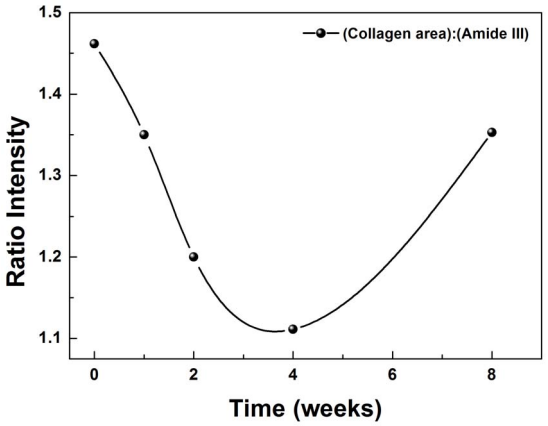

Figure 8. Comparison of area ratio (1340 cm^{-1}/1260 cm^{-1}) between mice non-infected liver tissue (t = 0) and after one, two, four and eight weeks of *Paracoccidioides brasiliensis* infection.
doi:10.1371/journal.pone.0106256.g008

shown that *Swiss* mice are relatively resistant to Pb infection [42–44].

The formation of granuloma in experimental models and in humans depends on factors such as susceptibility or resistance to infection [45]. On the other hand, the disease development depends on the fungus virulence and antigenic composition, on the environmental conditions and the immune response of the host [46].

In a previous study using the same kind of murine species, the evolution of granulomas in the lungs [37] was morphologically evaluated over 1, 2, 4 and 8 weeks after infection by Pb. Over time, the pulmonary granulomas became more numerous, larger and more organized, with increasing amounts of collagen fibers and reticulars [37]. Contrastingly, in the liver, the number of granulomas was greater in the first two weeks of infection and declined significantly by the eighth week. Furthermore, granulomas became smaller over time and did not develop significant fibrosis.

For the first time, expression of gp43 was evaluated by immunohistochemical staining in the livers of infected animals. Glycoprotein gp43 is the main antigenic component used for the diagnosis of PCM [10]. The immunostaining of gp43 in the liver

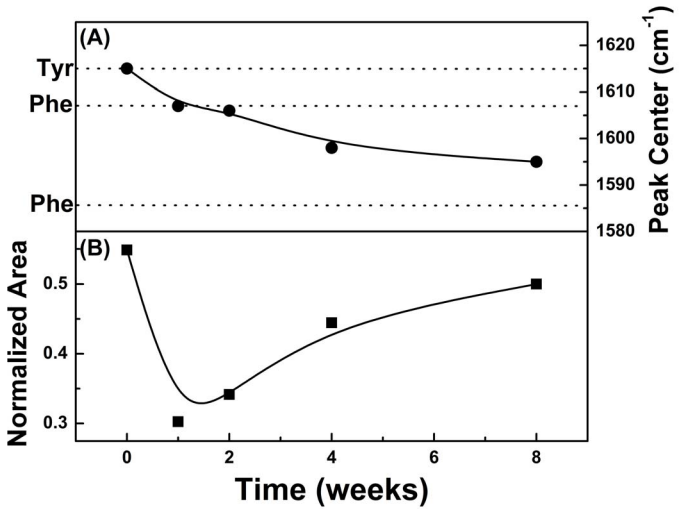

Figure 9. (A) Shifting of 1615 cm^{-1} peak position observed in non-infected liver (t = 0) toward low frequencies as a function of time infection. (B) Behavior of amino acids band area (1710-1510 cm^{-1}) as a function of time infection.
doi:10.1371/journal.pone.0106256.g009

was predominantly diffuse, with cytoplasmic and nuclear expression and in some yeast forms intact and fragmented. The staining intensity remained similar throughout the experimental period.

The gp43 may be synthesized and stored in dense vesicles that appear to migrate to the outer edge of the fungal cell wall, and are excreted extracellularly. Gp43 was detected in the cytoplasm of the macrophages in the fungal cell wall, in the host cells cytoplasm as well as in a dispersed manner [41].

The present study used a physical chemical evaluation which may represent a new alternative for diagnosis of PCM, namely FT-Raman spectroscopy. Raman spectroscopy is a method that, combined with histopathological analysis, can aid diagnosis, and has been most commonly employed in cancerous cells and tissue [47–50]. It provides detailed information of the biomolecular composition of tissues, allowing normal tissues to be distinguished from diseased tissues [17]. There are no studies in existing literature of spectral analysis of the livers of *Swiss* mice infected with Pb.

Since liver is not the target organ of Pb, few studies have linked infection by this microorganism with hepatic damage. The analysis via FT-Raman suggested that the infection caused structural and functional changes in the organ. Figure 8 shows a change in the spectral region related to the protein collagen [27,29]. The detected decrease of the collagen ratio, after the first week of infection, could be related to the Pb capacity to degrade the extracellular matrix, to adhere and to invade the host tissues. This process involves the interaction of the fungus with extracellular matrix proteins (ECM), such as enolase and adhesins. Adhesins are adhesion proteins in the Pb, which determine the binding capacity of this microorganism to matrix components such as collagen type I and IV, fibronectin, fibrinogen, and laminin [51], and also determine tropism by a cell or tissue [52,53]. In turn, the enolase acts as a plasminogen receptor with proteolytic capacity, contributing to the degradation of the ECM and the establishment of the fungus in the host [7] body.

On the other hand, the increase in the collagen ratio from the fourth to the eighth week can be related to the chronicity of the infection. In the lung, Pb target organ, the PCM evolved into fibrosis, which is characterized by matrix deposition and collagen accumulation [35]. In the liver, there was the development of a typical case of fibrosis, but a larger amount of collagen fibers, stained with Sirius red, was observed with the progression of the infection. Fibrosis is an intrinsic mechanism to stop the evolution of the microorganism, allowing the establishment of an apparent balance between the host and the parasite, as the fungus cannot be eradicated, since the treatments only decrease the amount of fungi in the body maintaining the risk of late reactivation [2,3]. In pediatric patients, the hepatic involvement is common and is related to a worse prognosis and a higher number of deaths. In these patients the amount of fungi present in the liver was associated with the intensity of fibrosis [36].

From a functional point of view, the infection seems to have influenced the amino acids metabolism. In the non-infected organs, no physicochemical changes were detected. In these animals a characteristic band of tyrosine amino acid has been identified (1615 cm^{-1}). In Figure 9 (A), in the infected organ, there was a detection peak displacement from 1615 cm^{-1} to 1595 cm^{-1}, related to tyrosine and phenylalanine, respectively, [28]. In the specific case of the conversion of phenylalanine to tyrosine, by phenylalanine hydroxylase, there is the incorporation of -OH radicals to the aromatic ring of phenylalanine, causing a rearrangement of loads in the ring, and consequently a peak displacement.

Figure 9 (B) shows the total area of the analyzed amino acid band, including tyrosine and phenylalanine (1710-1510 cm^{-1}). The variation of the area may be related to the Pb virulence. The decrease in the amino acid content in the first week, compared to the control tissue, may be related to the use of tyrosine by Pb to synthesize melanin, a mechanism that increases its resistance to antifungal activities of macrophages [54–56] making it more resistant to the host immune system. The increase in the area after the second week of infection indicates the occurrence of a reaction of the body against Pb. Nevertheless it was observed that this increase is accompanied by a peak displacement in the region of 1595 cm^{-1}, indicating a reduction in the hydroxylation process of phenylalanine.

The conversion of phenylalanine to tyrosine may have been affected by the reduction of the enzyme phenylalanine hydroxylase activity, an event that would explain such displacement detected until the eighth week of observation, when still had development of small numbers of CFUs.

It has been concluded that there was a directly proportional relation between the number of CFU, the number of granulomas and the physicochemical changes in the liver infected with Pb, that is: (a) periods of increased liver infection were the first two weeks, when there was also the largest number of granulomas and CFUs (b) periods of higher molecular and histopathological changes also corresponded to periods of increased infection. It was not possible to correlate the expression of gp43 with the physicochemical and morphological changes since the expression was similar in all periods.

Author Contributions

Conceived and designed the experiments: LH TIES MLB. Performed the experiments: GRM ESBM EMM. Analyzed the data: AMN FS LH ESBM GRM EMM. Contributed reagents/materials/analysis tools: LH MLB TIES. Contributed to the writing of the manuscript: LH ESBM FS AMN MLB.

References

1. Coutinho ZF, Da Silva D, Lazéra M, Petri V, De Oliveira RM, et al. (2002) Paracoccidioidomycosis mortality in Brazil (1990–1995). Cad Saúde Pública. Rio de Janeiro 18(5): 1441–1454.
2. Villalobos-Duno H, San-Blas G, Paulinkevicius M, Sanchez-Martin Y, Nino-Vega G (2013) Biochemical characterization of *Paracoccidioides brasiliensis* α-1,3-glucanase Agn1p, and its functionality by heterologous expression in Schzosaccharomyces pombe. PloS ONE 8(6): 1–12.
3. Shikanai-Yasuda MA, Telles Filho FQ, Mendes RP, Colombo AL, Moretti ML, et al. (2006) Consenso em paracoccidioidomicose – Relatório Técnico. Rev Soc Bras Med Trop 39(3): 297–310.
4. Pereira LA, Bao SN, Barbosa MS, Da Silva JLM, Felipe MSS, et al. (2007) Analysis of the *Paracoccidioides brasiliensis* triosephosphate isomerase suggests the potential for adhesion function. FEMS Yeast Res 7: 1381–1388.
5. Wanke B, Aidê MA (2009) Chapter 6 – Paracoccidioidomycosis. Continuing Education Course – Mycoses. J Bras Pneumol 35(12):1245–1249.
6. Nemecek JC, Wüthrich M, Klein BS (2006) Global control of dimorphism and virulence in fungi. Science 312: 583–588.
7. Nogueira SV, Fonseca FL, Rodrigues ML, Mundodi V, Abi-Chacra EA, et al. (2010) *Paracoccidioides brasiliensis* enolase is a surface protein that binds plasminogen and mediates interaction of yeast forms with host cells. Infect Immun 78(9): 4040–4050.
8. Pereira M, Bailão AM, Parente JA, Borges CL, Salem-Izacc SM, et al. (2009) Preferential transcription of *Paracoccidioides brasiliensis* genes: host niche and time-dependent expression. Mem Inst Oswaldo Cruz. Rio de Janeiro 104(3): 486–491.
9. Acorci MJ, Dias-Melicio LA, Golim MA, Bordon-Graciani AP, Peraçoli MTS, et al. (2008) Inhibition of human neutrophil apoptosis by *Paracoccidioides brasiliensis*: Role of interleukin-8. Scand J Immunol 69: 73–79.
10. Costa PF, Fernandes GF, dos Santos PO, Amaral CC, Camargo ZP (2010) Characteristics of environmental *Paracoccidioides brasiliensis*isolates. Mycopathologia 169: 37–46.

11. Nimrichter L, Rodrigues ML, Rodrigues EG, Travassos LR (2005) The multitude of targets for the immune system and drug therapy in the fungal cell wall. Microbes Infect 7: 789–798.
12. Vargas J, Vargas R (2009) Actualizaciones Paracoccidioidomicosis. Rev enferm infecc trop 1(1): 49–56.
13. Popi AF, Lopes JD, Mariano M (2002) Gp43 from *Paracoccidioides brasiliensis* inhibits macrophage functions. An evasion mechanism of the fungus. Cell Immunol 218: 87–94.
14. Rocha AA, Morais FV, Puccia R (2009) Polymorphism in the flanking regions of the PbGp43 gene from the human pathogen *Paracoccidioides brasiliensis*: search for protein binding sequences and poly (A) cleavage sites. BMC Microbiol 9: 277.
15. Bertoni TA, Perenha-Viana MCZ, Patussi EV, Cardoso RF, Svidzinski TIE (2012) Western blot is an efficient tool in differential diagnosis between paracoccidioidomycosis and pulmonary tuberculosis. ClinVaccine Immunol 19: 1–13.
16. Perenha-Viana MCZ, Gonzales IAA, Brockelt SR, Machado LNC, Svidzinski TIE (2012) Serological diagnosis of Paracoccidioidomycosis through a Western Blot technique. ClinVaccine Immunol 19(4): 616–619.
17. Lorincz AL, Haddad D, Naik R, Fung A, Cao A, et al. (2004) Raman spectroscopy for neoplastic tissue differentiation: A piloto study. J Pediatr Surg 39(6): 953–956.
18. De Paulo LF, Coelho AC, Svidzinski TIE, Sato F, Rohling JH, et al. (2013) Crude extract of Fusarium oxysporum induces apoptosis and structural alterations in the skin of healthy rats. J Biomed Optics 18(9): 0950041–9.
19. Moratto EM, Gutierrez RM, Sato F, Medina AN, Svidzinski TIE, et al. (2013) Morphological and structural changes in lung tissue infected by *Paracoccidioides brasiliensis*: FTIR Photoacoustic Spectroscopy and Histological Analysis. Photochem Photobiol Sci 89: 1170–1175.
20. Matos WB, Dos Santos GMC, Silva VEB, Gonçalves EGR, Silva AR (2012) Paracoccidioidomycosis in the State of Maranhão, Brazil: geographical and clinical aspects. Rev Soc Bras Med Trop 45(3): 385–389.
21. Nogueira MGS, Andrade GMQ, Tonelli E, Diniz SN, Goes AM, et al.(2006) Laboratory evolutive aspects of children under paracoccidioidomycosis treatment. Rev Soc Bras Med Trop 39(5): 478–483.
22. Takahachi G, Maluf MLF, Svidzinski TIE, Akimoto-Günther LS, Hübler MRNO, et al. (2006) Biochemical responses in mice experimentally infected with *Paracoccidioides brasiliensis* and treated with Canova. Braz Arch Biol Technol 49(6): 897–903.
23. Green CJ, Knight J, Precious S, Simpkin S (1981) Ketamine alone and combined with diazepam or xylazine in laboratory animals: a 10 year experience. Laboratory Animals 5: 163–170.
24. Restrepo A, Jiménez B (1980) Growth of *Paracoccidioides brasiliensis* yeast phase in a chemically defined culture medium. J Clin Microbiol 12 (2): 279–81.
25. Huppert M, Oliver DJ, Sun SH (1978) Combined methenamine-silver nitrate and hematoxylin & eosin stain for fungi in tissues. J Clin Microbiol 8(5): 598–603.
26. Grocott RG (1955) A stain for fungi in tissue sections and smears. Am J Clin Path 25: 975–979.
27. Huang N, Short M, Zhao J, Wang H, Lui H, et al. (2011) Full range characterization of the Raman spectra of organs in a murine model. Opt Express 23: 22892–22909.
28. Cheng W-T, Liu M-T, Liu H-N, Lin S-Y (2005) Micro-Raman spectroscopy used to identify and grade human skin pilomatrixoma. Microsc Res Tech 68: 75–79.
29. Aydin Ö, Kahraman M, Kiliç E, Çulha M (2009) Surface-enhanced Raman scattering of rat tissues. J Appl Spectrosc 63(6): 662–668.
30. Singer-Vermes LM, Burger E, Calich VLG, Modesto-Xavier LH, Sakamoto TN, et al. (1994) Pathogenicity of *Paracoccidioides brasilienis* isolates in the human disease and in an experimental murine model. Clin Exp Immunol 97: 113–119.
31. Borges-Walmsley MI, Chen D, Shu X, Walmsley A (2002) The pathobiology of *Paracoccidiodes brasiliensis*. Curr Trends Microbiol 10 (2): 80–87.
32. Barbosa W, Daher R, Oliveira AR (1968) Forma linfático-abdominal da Blastomicose Sul-Americana. Rev Inst MedTrop São Paulo 10(1): 16–27.
33. Brito T, Castro RM, Shiroma M (1968) Biopsia hepática na blastomicose sul-americana. Rev Inst Med Trop São Paulo 10(3): 188–191.
34. Bertini S, Colombo AL, Takahashi HK, Straus AH (2007) Expression of antibodies directed to Paracoccidioides brasiliensis glycosphingolipids during the course of Paracoccidioidomycosis treatment. Clin Vaccine Immunol 14(2): 150–156.
35. Bocalandro I, Albuquerque FJM (1960) Icterícia e comprometimento hepático na blastomicose sul-americana. A propósito de 10 casos. Rev Paul Med 56: 350–366.
36. Braga GM, Hessel G, Pereira RM, Escanhoela CA (2013) Hepatic involvement in pediatric patients with paracoccidioidomycosis: a histological study. Histopathology 64(2): 256–262.
37. Da Silva FC, Svidzinski TIE, Patussi EV, Cardoso CP, Dalalio MMO, et al. (2009) Morphologic organization of pulmonar granulomas in mice infected with *Paracoccidioides brasiliensis*. Am J Trop Med Hyg 80(5): 798–804.
38. Da Silva JF, Oliveira HC, Marcos CM, Da Silva RAM, Da Costa TA, et al. (2013) *Paracoccidoides brasiliensis* 30 kDa Adhesin: Identification as a 14-3-3 protein, cloning and subcellular localization in infection models. PloS ONE 8(4): 1–10.
39. González A, Lenzi HL, Motta EM, Caputo L, Restrepo A, et al. (2008) Expression and arrangement of extracellular matrix proteins in the lungs of mice infected with *Paracoccidioides brasiliensis* conidia. Int J Clin Exp Pathol 89: 106–116.
40. Mendes-Giannini MJS, Taylor ML, Bouchara JB, Burger E, Calich VLG, et al. (2000) Pathogegesis II: fungal responses to host responses: interaction of host cells with fungi. Med J Mycol 38: 113–123.
41. Hanna SA, Silva JLM, Mendes-Giannini MJS (2000) Adherence and intracellular parasitism of *Paracoccidioides brasiliensis* in vero cells. Microbes Infect 2: 887–884.
42. Defaveri J, Rezkallah-Iwasso MT, Franco MF (1982) Experimental pulmonar paracoccidioidomycosis in mice: Morphology and correlation of lesion with humoral and cellular immune response. Mycopathologia 77: 3–11.
43. Defaveri J, Martin LC, Franco M (1989) Histological and ultrastructural study of the inflammation evoked by *Paracoccidioides brasiliensis* antigen in previously immunized mice. Mycopathologia 105: 53–58.
44. Defaveri J, Rezkallah-Iwasso MT, Franco M (1992) Pulmonary paracoccidioidomycosis in immunized mice. Mycopathologia 119: 1–9.
45. Fortes RM, Kipnis A, Junqueira-Kipnis AP (2009) *Paracoccidioides brasiliensis* pancreatic destruction in *Calomyscallosus* experimentally infected. BMC Microbiol 9: 84.
46. Fortes MRP, Kurokawa CS, Marques AS, Miot HA, Marques MEA (2011) Immunology of paracoccidioidomycosis. An Bras Dermatol 86(3): 516–525.
47. Hawi SR, Campbell WB, Kajdacsy-Balla A, Murphy R, Adar F, et al. (1996) Characterization of normal and malignant human hepatocytes by Raman microespectroscopy. Cancer Lett 110(1–2): 35–40.
48. Malini R, Venkatakrishna K, Kurien J, Pai KM, Rao L, et al. (2006) Discrimination of normal, inflammatory, premalignant, and malignant oral tissue: A Raman spectroscopy study. Biopolymers 81(3): 179–193.
49. De Oliveira AF, Santos ID de AO, Cartaxo SB, Bitar RA, Simões MM, et al. (2010) Differential diagnosis in primary and metastatic cutaneous melanoma by FT-Raman spectroscopy. Acta Cir Bras 25(5):434–439.
50. Oshima Y, Shinzawa H, Takenaka T, Furihata C, Sato H (2010) Discrimination analysis of human lung cancer cells associated with histological type and malignancy using Raman spectroscopy. J Biomed Opt 15(1): 017009.
51. Andreotti PF, Monteiro S, Bailao AM, Soares CM, Benard G, et al. (2005) Isolation and partial characterization of a 30 kDa adhesin from *Paracoccidioides brasiliensis*. Microbes Infect 7: 875–881.
52. Mc Mahon JP, Wheat J, Sobel ME, Pasula R, Downing JF, et al. (1995) Murine laminin binds to *Histoplasma capsulatum*. A possible mechanism of dissemination. J Clin Infect Dis 96: 1010–1017.
53. Lenzi HL, Calich VLG, Mendes-Gianinni MJS, Xidieh CF, Miyaji M, et al. (2000) Two patterns of extracellular matrix expression in experimental paracoccidioidomycosis. Med. Mycol J 38: 115–119.
54. Da Silva MB, Thomaz L, Marques AF, Svidzinski AE, Nosanchuk JD, et al. (2009) Resistance of menalized yeast cells of *Paracoccidioides brasiliensis* to antimicrobial oxidants and inhibition of phagocytosis using carbohydrates and monoclonal antibody to CD18. Mem Inst Oswaldo Cruz 104(4): 644–648.
55. Da Silva MB, Marques AF, Nosanchuk JD, Casadevall A, Travassos LR, et al. (2006) Melanin in the dimorphic fungal pathogen *Paracoccidioides brasiliensis*: effects on phagocytosis, intracellular resistance and drug susceptibility. Microbes Infect 8: 197–205.
56. Apte M, Girme G, Bankar A, Ravikumar A, Zinjarde S (2013) 3,4-dihydroxy-L-phenylalanine-derived melanin from *Yarrowia lipolytica* mediates the synthesis of silver and gold nanostructures. J Nanobiotechnol 11(2):1–9.
57. Lien-Vien D, Colthup NB, Fateley WG, Grasseli JG (1991) The handbook of IR and Raman characteristic frequencies of organic molecules (Compounds containing $–NH_2$, –NHR and NR_2). Academic Press LTD California. pp. 155–175.
58. Socrates G (2001) Macromolecules in Infrared and Raman characteristic group frequencies. John Wiley & Son LTD Chichester. 366 p.